Journal of Alloys and Compounds 504 (2010) 377–381

Contents lists available at ScienceDirect

Journal of Alloys and Compounds

journal homepage: www.elsevier.com/locate/jallcom

Lower temperature fabrication of continuous intermetallic coatings on AZ91D magnesium alloy in molten salts

Cheng Zhong, Meifeng He*, Lei Liu, Yating Wu, Yujuan Chen, Yida Deng, Bin Shen, Wenbin Hu*

State Key Laboratory of Metal Matrix Composites, Shanghai Jiao Tong University, Shanghai 200240, China

ARTICLE INFO

Article history:
Received 5 April 2010
Received in revised form 17 May 2010
Accepted 25 May 2010
Available online 4 June 2010

Keywords:
Magnesium alloy
Molten salt
Diffusion
Corrosion
Hardness

ABSTRACT

A continuous Mg–Al intermetallic coating was fabricated on an AZ91D Mg alloy in molten salts in the lower temperature range from 300 °C up to 400 °C. The coating consists of a single $Mg_{17}Al_{12}$ intermetallic layer or both $Mg_{17}Al_{12}$ and Mg_2Al_3 intermetallic layers, depending on the treatment temperature. In contrast to the conventional powder pack cementation process, active Al atoms can be formed at a lower temperature in molten salts, which contributes to the lower temperature formation of continuous intermetallic layers. The intermetallic layer markedly improves the hardness as well as the corrosion resistance of the AZ91D Mg alloy. Furthermore, the continuous intermetallic layer exhibits passive behaviour in 3.5 wt.% NaCl solution, which is attributed to the homogenously distributed intermetallic phases.

1. Introduction

Mg alloys are advanced light structural and functional materials being increasingly used in the automotive, aerospace, electronic and energy industries, owing to their high strength-to-weight ratio, high thermal conductivity and electrical conductivity and good recycling with low energy consumption. However, the low corrosion resistance of Mg alloys is currently limiting their further applications [1]. Various surface modification techniques have been developed to improve the poor corrosion resistance of Mg alloys [2–6]. Of these techniques, recently developed surface alloying of Mg alloys by diffusion coating is of great interest because of the following potential advantages. Firstly, the electrical conductivity of the coated Mg alloy can be maintained. Moreover, the diffusion coating has high adhesion strength since there is a strong metallurgical bond between the coating and substrate [7]. In addition, the alloyed layer comprises of intermetallic compounds, which can both improve the corrosion resistance [8] and the mechanical properties [9].

Based on the above reasons, considerable research has been done trying to achieve diffusion coatings on Mg alloys [7,10–13]. For example, Shigematsu et al. [10] have obtained an Al-enriched diffusion coating by covering Mg alloys with Al powders at 450 °C. Al, Zn powder pack cementation and vacuum Al powder pack cementation have also been applied to obtain a diffusion coating reported by Ma et al. [7] and Liu et al. [12,13], respectively. Up to date, most of the work has used conventional powder pack cementation process and has to be carried out at high temperatures (near or even above the Mg–Al eutectic reaction temperature of 437 °C). However, such high temperatures may lead to surface melting and cracking, which will limit its applications for practical cases. Therefore, the major challenge for diffusion-alloyed coating of Mg alloys is to lower the treatment temperature in order to avoid the negative effects during the coating process [14].

Previous work from our group [15] has prepared intermetallic coatings on Mg alloys at a lower temperature of 420 °C through adding $ZnCl_2$ as activator; however, the formed intermetallic coating is not continuous and does not exhibit passive behaviour in aggressive NaCl solutions. Recently, Zhang et al. [16] have successfully lowered the diffusion coating temperature of AZ91D alloy to 380 °C by surface nanocrystallization of the substrate by surface mechanical attrition treatment (SMAT) first. Unfortunately, current SMAT techniques are not suitable for components with complex shapes.

Thus, the present work aims to develop a novel and simple process to prepare continuous Mg–Al intermetallic coatings with passive behaviour on AZ91D substrate at lower temperatures, without the need to pretreat the substrate specially. In this work, diffusion coating process of the AZ91D Mg alloy in a new system, i.e., molten salts containing aluminum ions, was studied. The hardness and the corrosion resistance of the coating were investigated by nanoindentation test and electrochemical measurements, respectively.

---

* Corresponding author. Tel.: +86 021 34202981; fax: +86 021 34202981.
E-mail addresses: hmf752@sjtu.edu.cn (M.F. He), wenbinhu@126.com (W.B. Hu).

0925-8388/$ – see front matter © 2010 Elsevier B.V. All rights reserved.
doi:10.1016/j.jallcom.2010.05.120

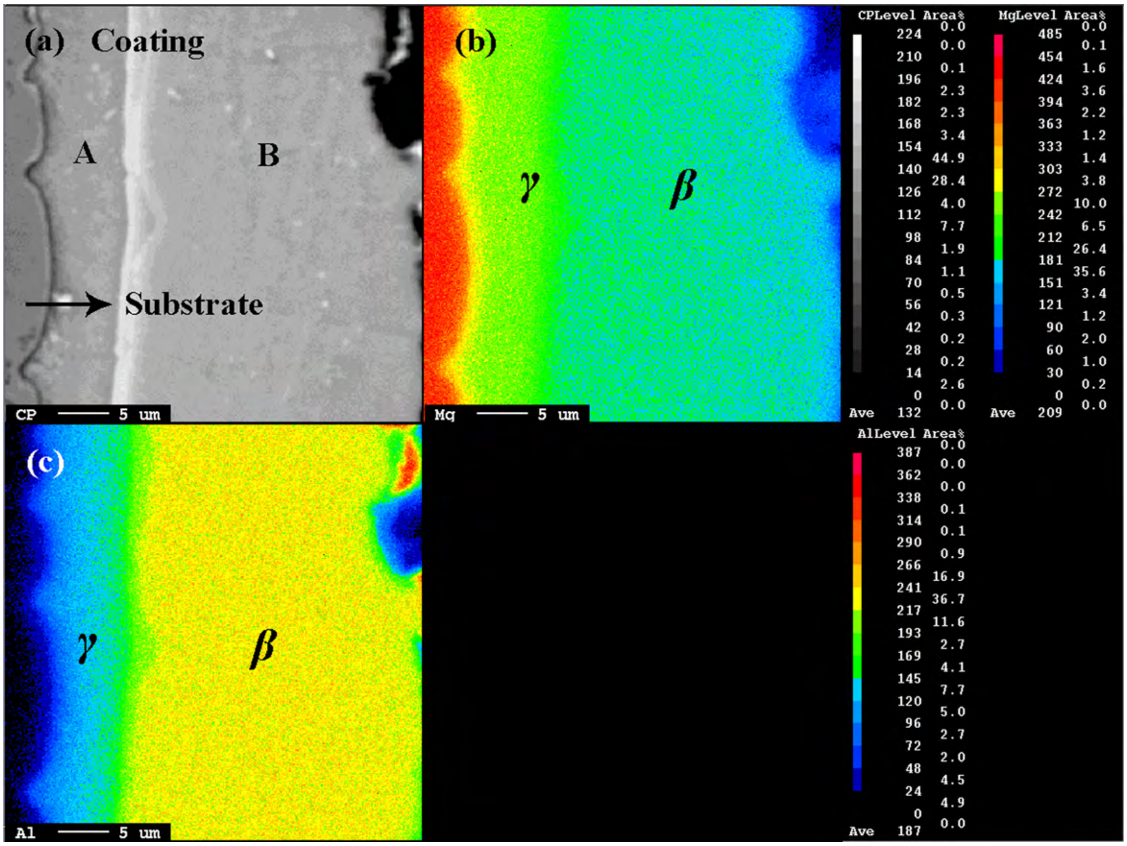

Fig. 1. Cross-sectional SEM micrographs of the (a) intermetallic coating on the AZ91D Mg alloy, EPMA-determined distribution of (b) Mg and (c) Al.

2. Experimental

An as-received AZ91D Mg alloy ingot was cut into 20 mm diameter × 10 mm long specimens and polished using up to 1000 grit SiC paper. The salt mixture containing 50% NaCl and 50% $AlCl_3$ (molar ratio) was selected for this study. The cleaned AZ91D specimens were put in the mixed salts in a ceramic container. An electric resistance furnace that can automatically control the temperature was employed to achieve the diffusion coating process, which was carried out in the temperature from 300 °C to 400 °C. During the whole process, protective pure argon gas (99.999%) was used to ensure the non-oxidation of the specimens.

The morphology and composition of the coated specimens were analyzed by a FEI SIRION-200 scanning electron microscopy (SEM), an X-ray energy dispersive spectrum (EDS) and a JSM-6700F electron probe microanalyzer (EPMA). Nanoindentation measurements were performed on the intermetallic layers and the substrate using a Hysitron Triboindenter. The maximum indentation load was 1000 μN. There was a stabilized time of 5 s between the loading and unloading stages.

The corrosion property of the specimens was investigated using a PARSTAT 2273 potentiostat. Potentiodynamic polarization measurements were conducted in a deaerated 3.5 wt.% NaCl solution at 25 °C. A classic three-electrode cell was used, with the test specimen as the working electrode, a platinum plate as the counter electrode, and a saturated calomel electrode (SCE) as the reference electrode. A polarization scan was started from a cathodic potential at a sweep rate of 0.33 mV/s and stopped when the anodic current reached 5 mA/cm^2.

3. Results and discussion

Fig. 1 shows a typical SEM image of the cross-section of an AZ91D specimen which is treated in molten salts at 400 °C for 6 h. Fig. 1(b) and (c) shows the corresponding distributions of Mg and Al, respectively obtained by EPMA mapping, and the right scale bars indicate the relative intensities of Mg and Al. It is seen that an obvious coating is formed on the surface of the substrate at a temperature that is much lower than the conventional powder pack cementation temperature. Three distinct zones can be observed, i.e., the inner layer of the coating (region A), outer layer of the coating (region B) and the substrate. Elemental mapping shows that Mg is enriched in the inner layer than the outer layer (Fig. 1(b)), while Al concentration in the outer layer is much higher than that in the inner layer (Fig. 1(c)). Furthermore, Fig. 1(b) and (c) shows no significant variations in the elemental concentrations at the same distance from the surface, indicating that Al and Mg are homogeneously distributed in the same depth of the layer. It is worth mentioning that most previously reported diffusion coatings are featured with a higher proportion of intermetallic phase than exists in the Mg matrix; few of them can prepare continuous intermetallic coatings. The difference will be further discussed later.

Fig. 2(a)–(c) shows typical SEM images of the cross-section of AZ91D specimens, which are treated in molten salts in the temperature range from 300 °C up to 400 °C. In addition, EDS elements line scanning along the yellow line in the cross-section of the treated AZ91D specimens are also given in Fig. 2. It is seen that the microstructure of the diffusion coating varies with the treatment temperature. An obvious coating is formed on the surface of the substrate at the temperature of 300 °C (Fig. 2(a)). As shown in Fig. 2(b), after treatment at 350 °C, the total thickness of the coating increases and two subzones can be observed in the coating, i.e., an inner dark grey layer (marked as “A”) and an outer light grey-coloured layer (marked as “B”). This suggests that the coating is composed of different phases, which will be clearly illustrated later by quantitative EDS analysis. When the treatment temperature increases to 400 °C, the thickness of the coating keeps increasing and it is interesting to note that the outer layer of the coating grows faster than the inner layer of the coating (Fig. 2(c)). Besides, EDS elements line scanning spectrum show that the concentration of Al decreases while Mg content increases with the increasing distance from the treated surface of the specimens (Fig. 2(a)–(c)). And the concentration of Mg and Al keeps constant in the substrate. It is

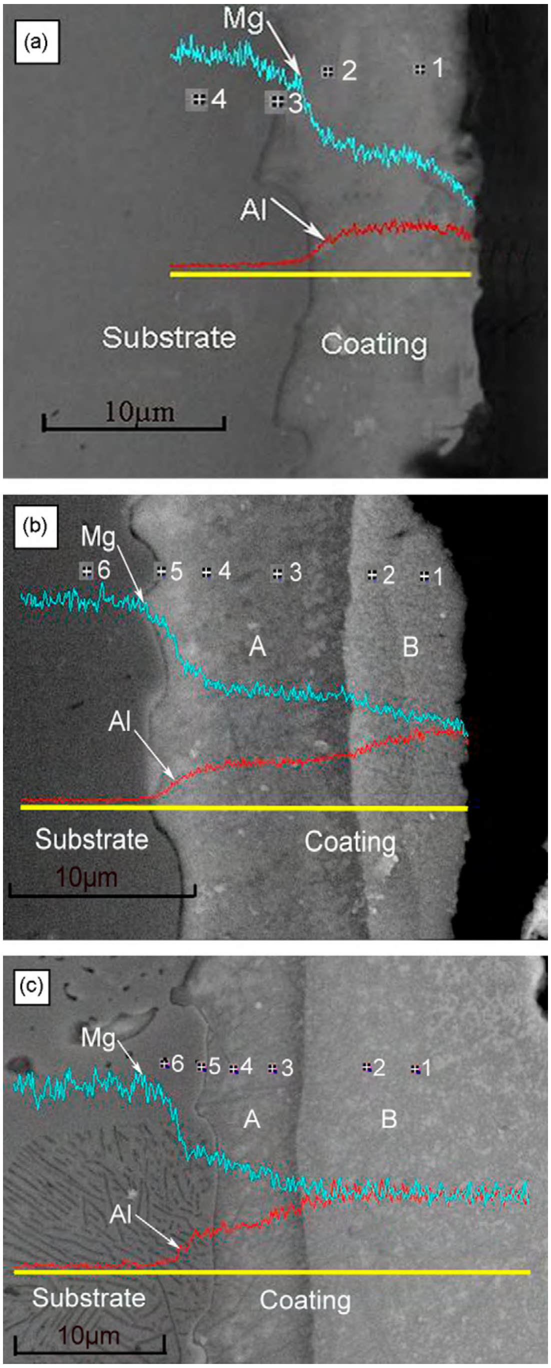

Fig. 2. SEM micrographs and corresponding EDS elements line scanning spectrums of the cross-section of the treated AZ91D specimens in molten salts (Mg: magnesium element; Al: aluminum element) at (a) 300 °C; (b) 350 °C; (c) 400 °C.

Table 1
Atomic ratios (at.%) of Mg and Al corresponding to the marked positions in Fig. 2(a).

Location	Mg (at.%)	Al (at.%)	Corresponding phase
1	52.42	47.58	γ-$Mg_{17}Al_{12}$
2	61.85	38.15	γ-$Mg_{17}Al_{12}$
3	89.29	10.71	δ-Mg solid solution
4	91.13	8.87	Mg substrate

Table 2
Atomic ratios (at.%) of Mg and Al corresponding to the marked positions in Fig. 2(b).

Location	Mg (at.%)	Al (at.%)	Corresponding phase
1	39.72	60.28	β-Al_3Mg_2
2	40.61	59.39	β-Al_3Mg_2
3	53.92	46.08	γ-$Mg_{17}Al_{12}$
4	62.80	37.20	γ-$Mg_{17}Al_{12}$
5	88.33	11.67	δ-Mg solid solution
6	91.10	8.90	Mg substrate

clear that the interdiffusion between Mg and Al occurs during the diffusion coating treatment in molten salts.

Tables 1–3 list the quantitative analysis of the chemical composition obtained by EDS corresponding to the marked points in Fig. 2(a)–(c), respectively. According to the Mg–Al binary phase diagram [17], there exists mainly β-Mg_2Al_3 and γ-$Mg_{17}Al_{12}$ equilibrium phases under the investigated temperature (300–400 °C). The β phase Mg_2Al_3 has a narrow composition range of about 2–3% with Al content from 60 at.% to 62.5 at.%. The γ phase $Mg_{17}Al_{12}$ has a wide composition range with Al concentration from 37.7 at.% to 56.8 at.%. Thus, it is reasonable to assume that the diffusion coating formed in molten salts at 300 °C mainly comprises of γ-$Mg_{17}Al_{12}$ phase (Table 1). With further increase in the treatment temperature (350–400 °C), the results indicate the presence of two intermetallic compounds (Tables 2 and 3). It is seen that the Al concentration is higher than Mg in the outer layer (see rows 1 and 2 in Tables 2 and 3) and much more Mg than Al is contained in the inner layer of the coating (see rows 3 and 4 in Tables 2 and 3). Similarly, based on the Mg–Al phase diagram, it can be deduced by the Mg-to-Al atom ratio that the outer layer of the coating composes of Mg_2Al_3 phase layer and inner layer is $Mg_{17}Al_{12}$ phase layer. It can be finally concluded that a $Mg_{17}Al_{12}$ intermetallic layer is first formed on the substrate at lower temperature of 300 °C (Table 1). And then a second Mg_2Al_3 intermetallic layer is formed at higher treatment temperatures (350–400 °C), as listed in Tables 2 and 3. The results are fully consistent with the SEM and EPMA observations of the diffusion coatings formed at various temperatures (Figs. 1 and 2). Funamizu and Watanabe have pointed out that two intermediate phases, Mg_2Al_3 and $Mg_{17}Al_{12}$, were formed in the Al–Mg diffusion couple at 325–425 °C [18]. This two-layered coating in the present work is fully consistent with their studies. Besides, similar results have also been reported by another study on the diffusion couple of Mg–Al system [17] and the heat treatment of Al cold spray coatings on AZ91D substrate at 400 °C [9].

Rolland et al. proposed that $AlCl_3$ formed a complex ion, $AlCl_4{}^-$, in molten salts [19]:

$$AlCl_3 + NaCl \rightarrow NaAlCl_4 \tag{1}$$

Displacement reaction-related active Al deposition occurs during the treatment of the substrates in molten salts:

$$3Mg + 2NaAlCl_4 \rightarrow 2Al + 3MgCl_2 + 2NaCl \tag{2}$$

The Gibbs free energy of reaction (2) follows $\Delta G = -461997 + 5.071T$ (J/mol), which is far below zero under the investigated temperature. Al deposition leads to the diffusion of active Al atoms into the AZ91D substrate. At the early stage of the reaction diffusion process, active Al atoms diffuse from the molten salts into the surface of the substrate, driven by chemical gradient. As the diffusion process continues, the concentration of

Table 3
Atomic ratios (at.%) of Mg and Al corresponding to the marked positions in Fig. 2(c).

Location	Mg (at.%)	Al (at.%)	Corresponding phase
1	39.92	60.08	β-Al_3Mg_2
2	40.45	59.55	β-Al_3Mg_2
3	52.08	47.92	γ-$Mg_{17}Al_{12}$
4	56.52	43.48	γ-$Mg_{17}Al_{12}$
5	88.45	11.55	δ-Mg solid solution
6	90.95	9.05	Mg substrate

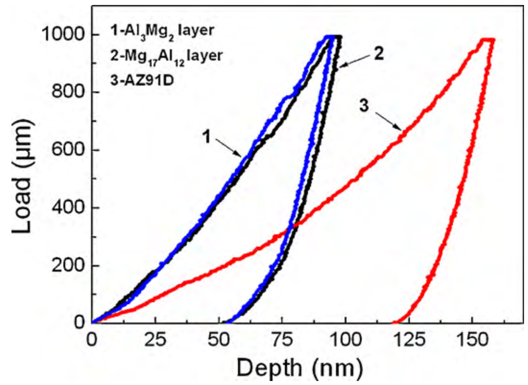

Fig. 3. Load–depth curves of the intermetallic coatings and the substrate.

Al in the top surface layer keeps rising. According to the Mg–Al phase diagram, once the Al concentration in the top surface exceeds the solid solubility of Al in Mg, the Al concentration dramatically increases and a γ-$Mg_{17}Al_{12}$ phase layer is first formed at the surface layer (see "γ" in Fig. 1). Similarly, with the further increasing Al concentration on the surface, the formation of a second β-Mg_2Al_3 phase layer at the top surface layer is observed (see "β" in Fig. 1). It can be seen that in this mode, active Al atoms can be formed at lower temperatures, which favors the following interdiffusion between Mg and Al, and consequently continuous Mg–Al intermetallic compounds are formed. On the contrary, in the case of conventional powder pack cementation process, it is difficult to form active Al atoms from Al powders at lower temperatures. Therefore, most of the previous work has to be carried out at high temperatures, and thus the $Mg/Mg_{17}Al_{12}$ eutectic reaction (437 °C) occurs, resulting in the formation of discontinuous intermetallic phases (i.e., α-Mg + γ-$Mg_{17}Al_{12}$).

Fig. 3 shows typical nanoindentation load–depth curves for the Al_3Mg_2 phase layer, $Mg_{17}Al_{12}$ layer, and AZ91D substrate. It is shown that the intermetallic layers have a significant smaller residual depth of penetration than that of the substrate, indicating their much higher hardness. The calculated hardness for the Al_3Mg_2 layer, $Mg_{17}Al_{12}$ layer and the substrate is 3.87 ± 0.3 GPa, 3.62 ± 0.3 GPa and 1.37 ± 0.1 GPa, respectively. The higher hardness of Mg–Al intermetallic compounds is due to the formation of covalent bonds in intermetallic compounds compared with the pure metals that are characterized by metallic bonds. The significant increase in the hardness of the intermetallic layers on the AZ91D alloy should be beneficial for the improvement of the wear resistance in service. In addition, since the bond between the intermetallic coating and the substrate is a diffusion bond, it will have high adhesion strength and should provide sufficient adhesion to resist pull-off [7,20].

Fig. 4 shows the potentiodynamic polarization curves of coated AZ91D (treated in molten salt at 400 °C for 6 h) and bare AZ91D alloy in 3.5% NaCl solution. The corrosion potential E_{corr} of the treated specimen is higher than that of the bare AZ91D specimen, indicating that the treated specimen is less active than the untreated AZ91D specimen. By fitting the polarization curves, it is found that the corrosion current density of the specimen decreases remarkably from 4.0×10^{-4} A/cm^2 to 1.4×10^{-5} A/cm^2 after diffusion coating process. Furthermore, it is interesting to note that bare AZ91D shows an activated-controlled anodic behaviour while coated AZ91D exhibits an obvious passive behaviour. Within the potential range of passivity, a very small anodic dissolution current, which is potential independent, is observed. It has been reported by previous literature that Mg–Al intermetallic compounds, including $Mg_{17}Al_{12}$ and Al_3Mg_2, exhibit spontaneous passivation in similar NaCl solutions [1,9]. The results of the present work are fully consistent with previous studies. However, it is worth noticing that that the Al-enriched coating obtained by conventional powder aluminizing at high temperatures from most of the previous work do not exhibit such expected passive behaviour. Based on the above discussion, it is reasonable to assume that the microstructure of the alloyed layer played an important role in passive behaviour. Most of the previously reported alloyed layers are featured with discontinuous intermetallic compounds. This inhomogeneous distribution of intermetallic compounds decreases the uniformity of the passive film, and thus would have a negative effect on the formation of passive film on the specimen. Therefore, in this study, the much enhanced corrosion resistance of coated AZ91D in aggressive NaCl solution is attributed not only to the formation of intermetallic compounds, but also to the more homogenously distributed intermetallic phases in the surface layer, which has been confirmed by SEM observation (Fig. 1(a)) and EPMA elemental mapping (Fig. 1(b) and (c)).

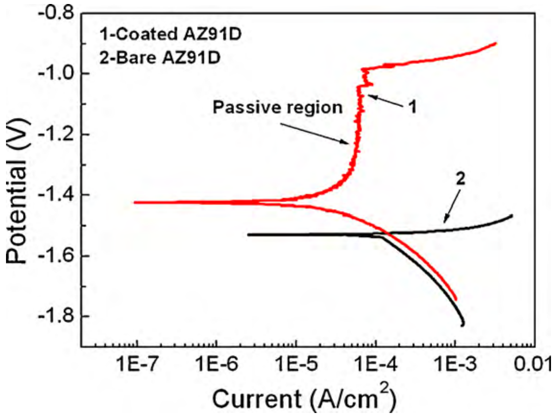

Fig. 4. Polarization curves of AZ91D Mg alloy with and without the intermetallic coating in 3.5 wt.% NaCl solution.

4. Conclusions

A continuous Mg–Al intermetallic coating is formed on the AZ91D Mg alloy by diffusion coating treatment in molten salts in the lower temperature range (300–400 °C). The intermetallic coating comprises of a $Mg_{17}Al_{12}$ phase layer or Mg_2Al_3 and $Mg_{17}Al_{12}$ phase layer, depending on the treatment temperature. The intermetallic coating greatly improves the hardness and the corrosion resistance of the AZ91D Mg alloys. Interestingly, the continuous intermetallic layers not only significantly decrease the corrosion current density of Mg alloys, but also exhibit a passive behaviour in NaCl solution, which is attributed to the homogenously distributed intermetallic phases. It is anticipated that this simple diffusion coating process in molten salts can be coupled with AZ91 solution heat treatment to produce protective intermetallic coatings on Mg alloys.

Acknowledgments

This work was supported by National Nature Science Foundation of China (No. 50974088), Cultural Fund for Major Program of Technology Innovation Engineering in Higher Education Institutions, China (No. 707025), Shanghai Rising-Star Program (No. 10QA1403400), Instrumental Analysis Center of Shanghai Jiao Tong University (IAC-SJTU).

References

[1] G.L. Song, Adv. Eng. Mater. 7 (2005) 563–586.
[2] J.E. Gray, B. Luan, J. Alloys Compd. 336 (2002) 88–113.
[3] R.C. Wolfe, B.A. Shaw, J. Alloys Compd. 437 (2007) 157–164.

[4] C.D. Gu, J.S. Lian, G.Y. Li, L.Y. Niu, Z.H. Jiang, J. Alloys Compd. 391 (2005) 104–109.
[5] M. Laleh, A. Sabour Rouhaghdam, T. Shahrabi, A. Shanghi, J. Alloys Compd., doi:10.1016/j.jallcom.2010.02.098.
[6] Ch. Christoglou, N. Voudouris, G.N. Angelopoulos, M. Pant, W. Dahl, Surf. Coat. Technol. 184 (2004) 149–155.
[7] Y.P. Ma, K.W. Xu, W.X. Wen, X.P. He, P.F. Liu, Surf. Coat. Technol. 190 (2005) 165–170.
[8] G.L. Song, A. Atrens, X.L. Wu, B. Zhang, Corros. Sci. 40 (1998) 1769–1791.
[9] K. Spencer, M.X. Zhang, Scripta Mater. 61 (2009) 44–47.
[10] I. Shigematsu, M. Nakamura, N. Saitou, K. Shimojima, J. Mater. Sci. Lett. 19 (2000) 473–475.
[11] J.S. Park, J.M. Kim, H.Y. Kim, J.S. Lee, I.H. Oh, C.S. Kang, Mater. Trans. 49 (2008) 1048–1051.
[12] F.C. Liu, W. Liang, X.R. Li, X.G. Zhao, Y. Zhang, H.X. Wang, J. Alloys Compd. 461 (2008) 399–403.
[13] F.C. Liu, X.R. Li, W. Liang, X.G. Zhao, Y. Zhang, J. Alloys Compd. 478 (2009) 579–585.
[14] H.Q. Sun, Y.N. Shi, M.-X. Zhang, K. Lu, Surf. Coat. Technol. 202 (2008) 3947–3953.
[15] M.F. He, Y.T. Wu, Z.X. Tang, W.B. Hu, J. Alloys Compd. 469 (2009) 417–421.
[16] M.X. Zhang, Y.N. Shi, H.Q. Sun, P.M. Kelly, J. Nanosci. Nanotechnol. 8 (2008) 2724–2728.
[17] C. Brubaker, Z.K. Liu, A.A. Luo (Eds.), Magnesium Technology 2004, Minerals, Metals and Materials Society/AIME, 184 Thorn Hill Road, Warrendale, PA, 2004, pp. 229–234.
[18] Y. Funamizu, K. Watanabe, Trans. JIM 13 (1972) 278–283.
[19] P. Rolland, G. Mamantov, J. Electrochem. Soc. 123 (1976) 1299–1303.
[20] M.-X. Zhang, H. Huang, K. Spencer, Y.N. Shi, Surf. Coat. Technol. 204 (2010) 2118–2122.